

# Light-cone path integral approach to the induced radiation in QED and QCD: basic concepts and recent applications

B.G. Zakharov <sup>a</sup>

<sup>a</sup> L.D. Landau Institute for Theoretical Physics, GSP-1, 117940, Kosygina Str. 2, 117334 Moscow, Russia

I discuss the basic ideas of the light-cone path integral approach to the induced radiation in QED and QCD and recent applications to the induced parton energy loss.

**1.** The induced radiative energy loss and the Landau-Pomeranchuk-Migdal (LPM) effect [1,2] in QED and QCD have attracted much attention in recent years, see [3,4,5] and references therein. It is mainly because of the first accurate measurements of the LPM effect in QED at SLAC [6], and the possibility to use jet quenching for probing the quark-gluon plasma (QGP) produced in high-energy  $AA$ -collisions [4,7,8,9]. The most general approach to the induced radiation applicable in both QED and QCD is the light-cone path integral (LCPI) approach [10] (see also [11,12,4]). It treats accurately the mass and finite-size effects, and applies at arbitrary strength of the LPM effect. This approach gives excellent description of the SLAC [6] and SPS [13] data on the photon radiation from high-energy electrons [14]. In this talk I discuss the basic concepts and recent applications of the LCPI approach.

**2.** The starting point of the LCPI formalism is the representation of the wave functions of high-energy free particles in the form (it is assumed that the angles between the  $z$  axis and velocities are small)

$$\psi_j(\mathbf{r}) = \exp(iE_j z) \hat{U}_j \phi_j(\boldsymbol{\rho}, z), \quad (1)$$

where  $\boldsymbol{\rho} = \mathbf{r}_\perp$ ,  $\hat{U}_j$  is a spin operator, and  $\phi_j$  satisfies the Schrödinger equation

$$i \frac{\partial \phi_j(\boldsymbol{\rho}, z)}{\partial z} = \left[ -\frac{1}{2\mu_j} \left( \frac{\partial}{\partial \boldsymbol{\rho}} \right)^2 + \frac{m_j^2}{2\mu_j} \right] \phi_j(\boldsymbol{\rho}, z). \quad (2)$$

The Schrödinger mass  $\mu_j$  in (2) equals the particle energy  $E_j$ . The  $z$ -evaluation of  $\phi_j$  is described



Figure 1.

by the Green's function for the Schrödinger equation (2),  $K_j$ . In vacuum the amplitude squared  $|\langle bc|T|a \rangle|^2$  for the  $a \rightarrow bc$  transition is given by the diagram shown in Fig. 1(a), where the  $\rightarrow$  ( $\leftarrow$ ) corresponds to  $K_j$  ( $K_j^*$ ), the dashed lines show the initial (at  $z_i \sim -\infty$ ) and final (at  $z_f \sim \infty$ ) transverse density matrices,  $\rho_i$ ,  $\rho_f$ , and the integration over the transverse coordinates of the endpoints (and vertices) and the longitudinal coordinates of the vertices (below  $z_1$  and  $z_2$  for upper and lower parts) is implicit. In vacuum  $\langle bc|T|a \rangle = 0$  (if the particle  $a$  is not produced in a hard reaction, and  $m_a \leq m_b + m_c$ ), however, in an external potential it is not the case.

To evaluate the induced  $a \rightarrow bc$  transition in an amorphous medium one should sum  $t$ -channel exchanges between the fast particles and particles in the medium and perform averaging over the medium states. The key idea of the LCPI approach is to represent all  $K_j$  in the Feynman path integral form, and perform averaging over the potential at the level of the integrands before integrating over the trajectories. After averaging over the medium states the interaction of the fast particles with the medium turns out to be translated to an effective interaction between trajectories. Both in QED and QCD from the point

of this interaction the trajectories corresponding to  $K_j^*$  may be viewed as antiparticle trajectories (below we call  $\rightarrow$  and  $\leftarrow$  lines “particle” and “antiparticle” trajectories). The effective Lagrangian reads

$$L_{eff} = L_0^p(\dot{\tau}_p) - L_0^{\bar{p}}(\dot{\tau}_{\bar{p}}) + L_{int}(\boldsymbol{\tau}_p, \boldsymbol{\tau}_{\bar{p}}), \quad (3)$$

where  $\boldsymbol{\tau}_p, \boldsymbol{\tau}_{\bar{p}}$  are the sets of the transverse coordinate for “particles” and “antiparticles”,  $L_0^p$  and  $L_0^{\bar{p}}$  are the corresponding free Lagrangians, say,  $L_0^p(\dot{\tau}_p) = \sum_i \mu_i \dot{\rho}_i^2/2$ . The interaction term reads  $L_{int}(\boldsymbol{\tau}_p, \boldsymbol{\tau}_{\bar{p}}) = in(z) \sigma_X(\boldsymbol{\tau}_p, \boldsymbol{\tau}_{\bar{p}})/2$ , where  $\sigma_X$  is the diffractive operator for  $X = \text{“particles”} + \text{“antiparticles”}$  system scattering off a particle in medium,  $n(z)$  is the number density of the medium. In QED  $\sigma_X$  is simply the cross section, but in QCD for the 4-body part ( $z_2 < z < z_f$ )  $\sigma_X$  acts as an operator in color space. The one-particle spectrum, say, integrated over  $\mathbf{q}_c$  (hereafter  $\mathbf{q}$  stands for the transverse momentum), may be represented in a form which does not contain the 4-body part at all. Since integration over  $\mathbf{q}_c$  gives  $\delta(\boldsymbol{\rho}_c - \boldsymbol{\rho}_{\bar{c}})$ , the diagram 1(a) is transformed into 1(b) in this case. The spectrum corresponding to the diagram 1(b) reads

$$\frac{dP}{dxd\mathbf{q}_b} = 2\text{Re} \int_{z_i}^{z_1} dz_1 \int_{z_1}^{z_f} dz_2 \times \hat{g} \langle \rho_f | \hat{S}_{b\bar{b}} \otimes \hat{S}_{bc\bar{a}} \otimes \hat{S}_{a\bar{a}} | \rho_i \rangle, \quad (4)$$

where  $x = x_b = p_{b,z}/p_{a,z}$ ,  $\hat{g}$  is the vertex factor,  $\hat{S}_{a\bar{a}}, \hat{S}_{b\bar{b}}, \hat{S}_{bc\bar{a}}$  are the evolution operators for the corresponding  $L_{eff}$ . For the two-body parts the path integrals can be taken analytically, say,

$$\langle \boldsymbol{\rho}'_a, \boldsymbol{\rho}'_{\bar{a}}, z' | \hat{S}_{a\bar{a}} | \boldsymbol{\rho}_a, \boldsymbol{\rho}_{\bar{a}}, z \rangle = K_a(\boldsymbol{\rho}'_a, z' | \boldsymbol{\rho}_a, z) \times K_{\bar{a}}^*(\boldsymbol{\rho}'_{\bar{a}}, z' | \boldsymbol{\rho}_{\bar{a}}, z) \Phi_{a\bar{a}}(\boldsymbol{\rho}'_a - \boldsymbol{\rho}'_{\bar{a}}, z' | \boldsymbol{\rho}_a - \boldsymbol{\rho}_{\bar{a}}, z), \quad (5)$$

where  $\Phi_{a\bar{a}} = \exp[-\frac{1}{2} \int_{\bar{z}}^z dz n(z) \sigma_{a\bar{a}}(\boldsymbol{\rho}_a(z) - \boldsymbol{\rho}_{\bar{a}}(z))]$  should be evaluated for the straight trajectories of  $a$  and  $\bar{a}$ . For the  $bc\bar{a}$ -part one can write  $\int D\boldsymbol{\rho}_b D\boldsymbol{\rho}_c D\boldsymbol{\rho}_{\bar{a}}$  as  $\int D\boldsymbol{\rho} D\boldsymbol{\rho}_a D\boldsymbol{\rho}_{\bar{a}}$ , where  $\boldsymbol{\rho} = \boldsymbol{\rho}_b - \boldsymbol{\rho}_c$ , and  $\boldsymbol{\rho}_a = x_b \boldsymbol{\rho}_b + x_c \boldsymbol{\rho}_c$  is the center-of-mass coordinate of the  $bc$  system. The  $\boldsymbol{\rho}_a$  and  $\boldsymbol{\rho}_{\bar{a}}$  integrals can be taken analytically, and in the new variables  $S_{bc\bar{a}}$  can be represented as

$$\langle \boldsymbol{\rho}'_a, \boldsymbol{\rho}'_{\bar{a}}, \boldsymbol{\rho}', z' | \hat{S} | \boldsymbol{\rho}_a, \boldsymbol{\rho}_{\bar{a}}, \boldsymbol{\rho}, z \rangle = K_a(\boldsymbol{\rho}'_a, z' | \boldsymbol{\rho}_a, z)$$

$$\times K_{\bar{a}}^*(\boldsymbol{\rho}'_{\bar{a}}, z' | \boldsymbol{\rho}_{\bar{a}}, z) \mathcal{K}(\boldsymbol{\rho}', z' | \boldsymbol{\rho}, z), \quad (6)$$

where  $\mathcal{K}$  is the Green’s function for the Hamiltonian

$$\hat{H} = -\frac{1}{2M(x)} \left( \frac{\partial}{\partial \boldsymbol{\rho}} \right)^2 + v(z, \boldsymbol{\rho}) + \frac{1}{L_f}, \quad (7)$$

where  $v(z, \boldsymbol{\rho}) = -in(z) \sigma_{bc\bar{a}}(\boldsymbol{\rho}, \boldsymbol{\rho}_a - \boldsymbol{\rho}_{\bar{a}})/2$  should be evaluated for the straight trajectories  $\boldsymbol{\rho}_a, \boldsymbol{\rho}_{\bar{a}}$ ,  $M(x) = E_a x (1-x)$ ,  $L_f = 2M(x)/\epsilon^2$  is the formation length,  $\epsilon^2 = [m_b^2 x_c + m_c^2 x_b - m_a^2 x_b x_c]$ . Having (5) and (6), one can obtain

$$\begin{aligned} \frac{dP}{dxd\mathbf{q}_b} = & \frac{2}{(2\pi)^2} \text{Re} \int d\boldsymbol{\tau} \exp(-i\mathbf{q}_b \cdot \boldsymbol{\tau}) \int_{z_i}^{z_f} dz_1 \\ & \times \int_{z_1}^{z_f} dz_2 \hat{g} \Phi_f(\boldsymbol{\tau}, z_2) \mathcal{K}(\boldsymbol{\tau}, z_2 | 0, z_1) \Phi_i(x\boldsymbol{\tau}, z_1), \quad (8) \\ \Phi_i(\boldsymbol{\tau}, z_1) = & \exp \left[ -\frac{\sigma_{a\bar{a}}(\boldsymbol{\tau})}{2} \int_{z_i}^{z_1} dz n(z) \right], \\ \Phi_f(\boldsymbol{\tau}, z_2) = & \exp \left[ -\frac{\sigma_{b\bar{b}}(\boldsymbol{\tau})}{2} \int_{z_2}^{z_f} dz n(z) \right]. \end{aligned}$$

The contribution stemming from the region of large  $|z_{1,2}|$  in (8) can be expressed via the light-cone wave-function of the  $a \rightarrow bc$  transition in vacuum,  $\Psi_a^{bc}$ , [4]. Then (8) takes the form

$$\begin{aligned} \frac{dP}{dxd\mathbf{q}_b} = & \frac{2}{(2\pi)^2} \text{Re} \int d\boldsymbol{\tau} \exp(-i\mathbf{q}_b \cdot \boldsymbol{\tau}) \\ & \times \int_{z_i}^{z_f} dz_1 \int_{z_1}^{z_f} dz_2 \hat{g} \{ \Phi_f(\boldsymbol{\tau}, z_2) [\mathcal{K}(\boldsymbol{\tau}, z_2 | 0, z_1) \\ & - \mathcal{K}_v(\boldsymbol{\tau}, z_2 | 0, z_1)] \Phi_i(x\boldsymbol{\tau}, z_1) \\ & + [\Phi_f(\boldsymbol{\tau}, z_2) - 1] \mathcal{K}_v(\boldsymbol{\tau}, z_2 | 0, z_1) [\Phi_i(x\boldsymbol{\tau}, z_1) - 1] \} \\ & - \frac{1}{(2\pi)^2} \int d\boldsymbol{\tau} d\boldsymbol{\tau}' \exp(-i\mathbf{q}_b \cdot \boldsymbol{\tau}) \Psi_a^{bc*}(x, \boldsymbol{\tau}' - \boldsymbol{\tau}) \\ & \times \Psi_a^{bc}(x, \boldsymbol{\tau}') [\Phi_f(\boldsymbol{\tau}, z_i) + \Phi_i(x\boldsymbol{\tau}, z_f) - 2], \quad (9) \end{aligned}$$

where  $\mathcal{K}_v$  is the Green’s function for  $v = 0$ . For  $L_f \gg L$  ( $L$  is the thickness of the medium) using the representation of  $\Psi_a^{bc}$  via the  $z$ -integral of  $\mathcal{K}$  established in [15] one can represent (9) as

$$\begin{aligned} \frac{dP}{dxd\mathbf{q}_b} = & \frac{1}{(2\pi)^2} \text{Re} \int d\boldsymbol{\tau} d\boldsymbol{\tau}' \exp(-i\mathbf{q}_b \cdot \boldsymbol{\tau}) \\ & \times \Psi_a^{bc*}(x, \boldsymbol{\tau}' - \boldsymbol{\tau}) \Psi_a^{bc}(x, \boldsymbol{\tau}') \\ & \times [2\Gamma_{bc\bar{a}}(\boldsymbol{\tau}', x\boldsymbol{\tau}) - \Gamma_{b\bar{b}}(\boldsymbol{\tau}) - \Gamma_{a\bar{a}}(x\boldsymbol{\tau})], \quad (10) \end{aligned}$$

where  $\Gamma_h = 1 - \exp[-\frac{\sigma_h}{2} \int_{-\infty}^{\infty} dz n(z)]$ .

From (9) one obtains for the  $x$ -spectrum

$$\frac{dP}{dx} = 2\text{Re} \int_{z_i}^{z_f} dz_1 \int_{z_1}^{z_f} dz_2 \hat{g} [\mathcal{K}(\rho_2, z_2 | \rho_1, z_1) - \mathcal{K}_v(\rho_2, z_2 | \rho_1, z_1)] \Big|_{\rho_1=\rho_2=0}. \quad (11)$$

In [15], separating the  $N = 1$  rescattering, we have represented (11) as a sum of the Bethe-Heitler spectrum plus an absorptive correction responsible for the LPM effect. This form has been used [14] for successful description of the SLAC [6] and SPS [13] data on the LPM effect in photon bremsstrahlung from high energy electrons.

For a particle produced in the medium it is convenient to rewrite (11) in another form. For gluon emission from a quark this new form reads [16]

$$\frac{dP}{dx} = \int_0^L dz n(z) \frac{d\sigma_{eff}^{BH}(x, z)}{dx}, \quad (12)$$

$$\frac{d\sigma_{eff}^{BH}(x, z)}{dx} = \text{Re} \int_0^z dz_1 \int_z^\infty dz_2 \int d\rho \hat{g} \times \mathcal{K}_v(\rho_2, z_2 | \rho, z) \sigma_3(\rho) \mathcal{K}(\rho, z | \rho_1, z_1) \Big|_{\rho_1=\rho_2=0}, \quad (13)$$

where  $\sigma_3 = \sigma_{gq\bar{q}}$ ,  $L$  is the quark pathlength in the medium. The  $d\sigma_{eff}^{BH}/dx$  (13) can be viewed as an effective Bethe-Heitler cross section which accounts for the LPM and finite-size effects. Neglecting spin-flip transition (13) can be written as

$$\frac{d\sigma_{eff}^{BH}(x, z)}{dx} = -\frac{\alpha_s P_q^{gg}(x)}{\pi M(x)} \times \text{Im} \int_0^z d\xi \frac{\partial}{\partial \rho} \left( \frac{F(\xi, \rho)}{\sqrt{\rho}} \right) \Big|_{\rho=0}, \quad (14)$$

where  $P(x)_q^{gg} = C_F[1 + (1 - x)^2]/x$  is the usual splitting function, and  $F$  is the solution of the radial Schrödinger equation for the azimuthal quantum number  $m = 1$

$$i \frac{\partial F(\xi, \rho)}{\partial \xi} = \left[ -\frac{1}{2M(x)} \left( \frac{\partial}{\partial \rho} \right)^2 - i \frac{n(z - \xi) \sigma_3(\rho)}{2} + \frac{4m^2 - 1}{8M(x)\rho^2} + \frac{1}{L_f} \right] F(\xi, \rho). \quad (15)$$

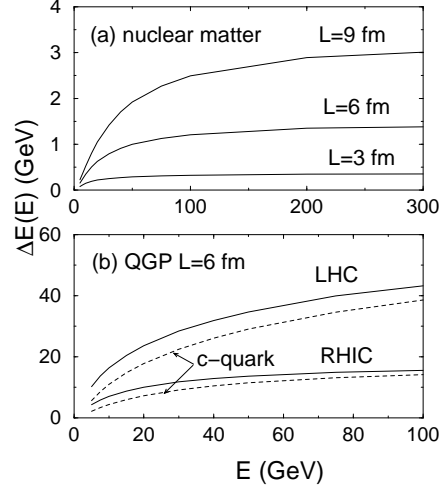


Figure 2. The quark energy loss in the nuclear matter (a) for  $L = 3, 6, 9$  fm and expanding QGP (b) for  $L = 6$  fm for RHIC and LHC.

The boundary condition for  $F(\xi, \rho)$  reads  $F(\xi = 0, \rho) = \sqrt{\rho} \sigma_3(\rho) \epsilon K_1(\epsilon \rho)$ , where  $K_1$  is the Bessel function.

3. The formulas (12), (14) are convenient for numerical calculations with an accurate parametrization of  $\sigma_3$ . Note that the widely used oscillator approximation  $\sigma_3(\rho) \propto \rho^2$  is too crude for the induced gluon emission [17,16]. We perform calculations for running  $\alpha_s$  frozen at the value 0.7 for small virtuality (for incorporation of running  $\alpha_s$  see [16]). In Fig. 2 we show the energy dependence of the quark energy loss  $\Delta E = E \int dx x dP/dx$  for the cold nuclear matter and for expanding QGP for RHIC and LHC conditions. For nuclear matter we take  $m_g = 0.75$  GeV obtained from the analysis of the low- $x$  proton structure function within the dipole BFKL equation [18,19]. It agrees well with the inverse gluon correlation radius in the QCD vacuum [20]. For QGP we use  $m_g = 0.4$  obtained in the quasi-particle model from the lattice data in [21]. For the light quark we take  $m_q = 0.3$ . For QGP this quark mass was obtained in [21]. Note that our results are not very sensitive to the light quark mass. For the QGP we also show the results for

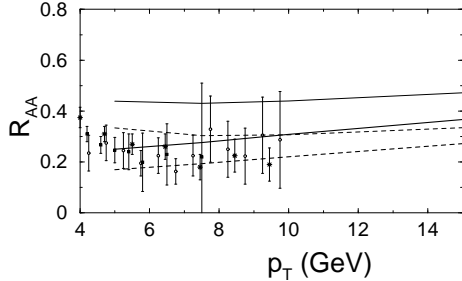


Figure 3. The nuclear modification factor for central  $Au + Au$  collisions at  $\sqrt{s} = 200$  GeV for quark (solid line) and gluon (dashed line) jets obtained with  $m_g = 0.4$  GeV (thick lines) and  $m_g = 0.75$  GeV (thin lines). The experimental points (from [26]) are for: circle -  $Au + Au \rightarrow \pi^0 + X$  (0-10% central) [PHENIX Collaboration], square -  $Au + Au \rightarrow h^\pm + X$  (0-10% central) [PHENIX Collaboration], star -  $Au + Au \rightarrow h^\pm + X$  (0-5% central) [STAR Collaboration].

$c$ -quark,  $m_q = 1.5$  GeV. The Debye screening mass,  $\mu_D$ , in QGP was obtained from the perturbative relation  $\mu_D = \sqrt{2}m_g \approx 0.57$  GeV. We use the Bjorken model for the QGP expansion with  $T^3\tau = T_0^3\tau_0$  and the initial conditions suggested in [23]:  $T_0 = 446$  MeV and  $\tau_0 = 0.147$  fm for RHIC (for  $Au + Au$  at  $\sqrt{s} = 200$  GeV), and  $T_0 = 897$  MeV and  $\tau_0 = 0.073$  fm for LHC ( $Pb + Pb$  at  $\sqrt{s} = 5.5$  TeV). For the QGP we take  $L = 6$  fm. It is about the life-time of the QGP (and mixed) phase for central heavy-ion collisions, since due to the transverse expansion the hot QCD matter should cool quickly at  $\tau \gtrsim \tau_{max} \sim R_A$ .

$\Delta E$  for nuclear matter obtained using (12)-(15) with an accurate parametrization of the imaginary potential by a factor of about 2 smaller than that obtained previously [9] in the oscillator approximation. Our  $\Delta E$  for nuclear matter is considerably smaller than prediction of [24] in the HERMES [25] energy region  $E \lesssim 20$  GeV. The small  $\Delta E$  shows that for the HERMES conditions the effects of hadron absorption and string tension should be more important than the gluon emission since the hadron formation time  $l_f$  is about the nuclear size. Note that the estimate

$l_f \sim 40$  fm for  $E = 8$  GeV given in [24] is absolutely unrealistic. The authors of [24] do not pay any attention to the fact that a quark with such an energy should be stopped at  $L \lesssim 8$  fm since the string tension is  $\sim 1$  GeV/fm.

One can see from Fig. 2b that for LHC conditions the jets with  $E \lesssim 20$  GeV should practically be absorbed in the QGP. It means that the surface jet production dominates. The energy loss for  $c$ -quark is smaller than that for light quarks by a factor of  $\sim 2$  at  $E \sim 5 - 10$  GeV.

The effect of parton energy loss on the high- $p_T$  hadron production in  $A + A$  collisions can approximately be described in terms of effective hard partonic cross sections which account for the induced gluon emission [8]. Using the power-low parametrization for cross section of quark production in  $p + p$  collisions  $\propto 1/p_T^{n(p_T)}$  the nuclear modification factor

$$R_{AA}(p_T) = \frac{d\sigma^{AA}(p_T)/dydp_T^2}{N_{bin}d\sigma^{pp}(p_T)/dydp_T^2} \quad (16)$$

can be written as [16]

$$R_{AA}(p_T) \approx P_0(p_T) + \frac{1}{J(p_T)} \int_0^1 dz z^{n(p_T)-2} D_q^h(z, \frac{p_T}{z}) \times \int_0^1 dx (1-x)^{n(p_T)/z-2} \frac{dI(x, \frac{p_T}{z(1-x)})}{dx}, \quad (17)$$

where  $J(p_T) = \int_0^1 dz z^{n(p_T)-2} D_q^h(z, \frac{p_T}{z})$ ,  $P_0$  is the probability of quark propagation without induced gluon emission,  $dI(x, p_T)/dx$  is the probability distribution in the quark energy loss for a quark with  $E = p_T$ ,  $D_q^h(z, p_T/z)$  is the quark fragmentation function. A convenient parametrization for  $P_0$  and  $dI(x, p_T)/dx$  in terms of  $dP/dx$  (similar to that used for photon emission in [14]) is given in [16]. In Fig. 3 we compare the theoretical  $R_{AA}$  with the RHIC data on  $Au + Au$  collisions at  $\sqrt{s} = 200$  GeV [26]. The theoretical curves have been obtained for  $L = 4.9$  fm. It is the typical parton pathlength in the QGP (and mixed) phase for  $\tau_{max} = 6$  fm. The results for the quark and gluon jets are shown separately (for  $\sqrt{s} = 200$  GeV the quark and gluon contributions are comparable). The suppression is somewhat stronger for gluon jets. As for Fig. 2(b) the calculations are

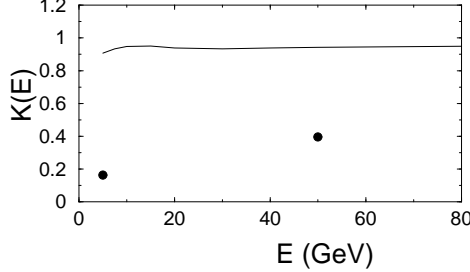


Figure 4. The kinematic  $K$ -factor for  $N = 1$  rescattering for the QGP,  $L = 5$  fm,  $n(z) = \text{const.}$  Solid line shows our results. The points show the GLV [7] predictions.

performed for  $m_q = 0.3$  GeV and  $m_g = 0.4$  GeV. To illustrate the  $m_g$ -dependence we also show the results for  $m_g = 0.75$  GeV (with the same  $\mu_D$  as for  $m_g = 0.4$  GeV), which seems to be reasonable for the mixed phase and for gluons with large formation length  $L_f \gtrsim L$ . The above two values of  $m_g$  give reasonable lower and upper limits of the infrared cutoff for the induced gluon emission for RHIC conditions. The theoretical  $R_{AA}$  for  $m_g = 0.4$  is in quite good agreement with the experimental one.

4. The LCPI approach neglects the kinematic bounds. The GLV group [7] reported that the finite kinematic limits suppress strongly the energy loss even at  $E \sim 500$  GeV. To check it in [22] we have calculated the dominating  $N = 1$  rescattering contribution to the quark energy loss using the ordinary diagram language. We have obtained a small kinematic effect. To demonstrate it in Fig. 4 we show the kinematic  $K$ -factor  $K = \Delta E_{f.l.}/\Delta E_{i.l.}$ , where  $\Delta E_{f.l.}$  and  $\Delta E_{i.l.}$  are the energy losses for finite and infinite kinematic limits. Our calculations are performed for the kinematic limits as in [7], also similarly to [7] we use fixed  $\alpha_s$ ,  $n(z) = \text{const}$ ,  $L = 5$  fm, and  $m_g = \mu_D = 0.5$  GeV. One sees that our  $K$ -factor contrary to the GLV predictions is close to unity even for  $E \sim 5$  GeV. It says that the LCPI approach has a quite good accuracy for  $E \gtrsim 5$  GeV.

I thank the Organizers of Diffraction'04 for the hospitality and financial support during the Workshop.

## REFERENCES

1. L.D. Landau and I.Ya. Pomeranchuk, Dokl. Akad. Nauk SSSR **92** (1953) 535, 735.
2. A.B. Migdal, Phys. Rev. **103** (1956) 1811.
3. S.R. Klein, Rev. Mod. Phys. **71** (1999) 1501.
4. R. Baier, D. Schiff and B.G. Zakharov, Ann. Rev. Nucl. Part. **50** (2000) 37.
5. A. Kovner and U.A. Wiedemann, hep-ph/0304151.
6. P.L. Anthony, R. Becker-Szendy, P.E. Bosted, et al., Phys. Rev. D**56** (1997) 1373.
7. M. Gyulassy, P. Lévai and I. Vitev, Nucl. Phys. B**594** (2001) 371.
8. R. Baier, Yu.L. Dokshitzer, A.H. Mueller and D. Schiff, JHEP **0109** (2001) 033.
9. B.G. Zakharov, JETP Lett. **65** (1997) 615.
10. B.G. Zakharov, JETP Lett. **63** (1996) 952.
11. B.G. Zakharov, Phys. Atom. Nucl. **61** (1998) 838.
12. B.G. Zakharov, JETP Lett. **70** (1999) 176.
13. H.D. Hansen, U.I. Uggerhøj, C. Biino et al., Phys. Rev. Lett. **91** (2003) 014801.
14. B.G. Zakharov, Phys. Atom. Nucl. **62** (1999) 1008; JETP Lett. **78** (2003) 759.
15. B.G. Zakharov, JETP Lett. **64** (1996) 781.
16. B.G. Zakharov, hep-ph/0410321.
17. B.G. Zakharov, JETP Lett. **73** (2001) 49.
18. N.N. Nikolaev, B.G. Zakharov and V.R. Zoller, Phys. Lett. B**328** (1994) 486.
19. N.N. Nikolaev and B.G. Zakharov, Phys. Lett. B**327** (1994) 149.
20. E.V. Shuryak, Rev. Mod. Phys. **65** (1993) 1.
21. P. Lévai and U. Heinz, Phys. Rev. C**57** (1998) 1879.
22. B.G. Zakharov, JETP Lett. **80** (2004) 67.
23. R.J. Fries, B. Müller and D.K. Srivastava, Phys. Rev. Lett. **90** (2003) 132301.
24. E. Wang and X.N. Wang, Phys. Rev. Lett. **89** (2002) 162301.
25. A. Airapetian et al. (HERMES Collaboration), Phys. Lett. B**577** (2003) 37.
26. D. d'Enterria, Invited overview talk at 39th Rencontres de Moriond on QCD and High-Energy Hadronic Interactions, La Thuile, Italy, 28 Mar - 4 Apr 2004; nucl-ex/0406012.